



# KINETICS OF CORROSION CRACK GROWTH IN 17G1S PIPE STEEL

V.I. MAKHNENKO, L.I. MARKASHOVA, E.N. BERDNIKOVA, V.M. SHEKERA and E.M. ONOPRIENKO  
E.O. Paton Electric Welding Institute, NASU, Kiev, Ukraine

Relationship between the rate of growth of corrosion cracks and stress intensity factor was described on the basis of the static corrosion crack resistance diagram. The main working hypothesis that crack growth is of a discrete nature was proved by means of analytical scanning microscopy.

**Keywords:** pipe steels, corrosion cracks, diagram of static corrosion resistance, acoustic emission, electron microscopy, hydrogen embrittlement zone

Corrosion cracks in underground main gas and oil pipelines are the most hazardous defects, which are quite difficult to detect using modern means of in-pipe diagnostics. In this connection, studying the above defects in terms of their initiation and development certainly is of great interest, particularly for specialists, dealing with pipeline repair without taking them out of service, i.e. under pressure, when ranking the detected defects by the urgency of their repair is a critical component of the repair schedule.

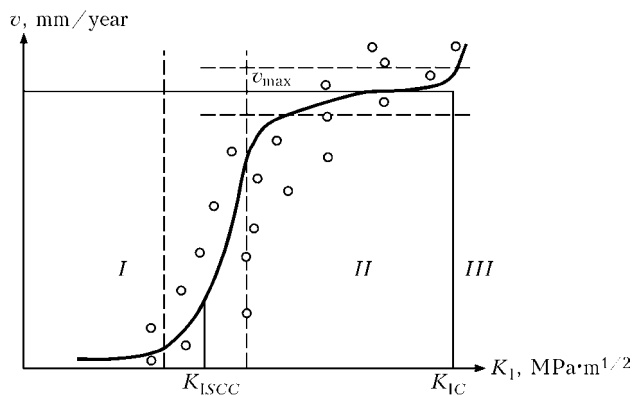


Figure 1. Diagram of static corrosion crack resistance (I-III, as well as other designations see in the text)

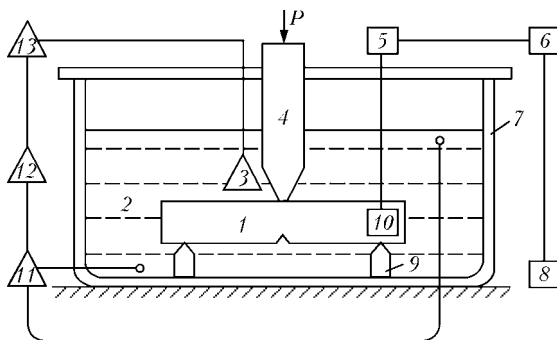


Figure 2. Schematic of sample testing in a pilot unit developed at PWI: 1 – sample; 2 – corrosion medium; 3 – medium temperature sensor; 4 – indenter; 5 – amplifier; 6 – acoustic emission source; 7 – pool; 8 – registering device; 9 – support; 10 – piezoelectric transducer; 11 – medium circulating pump; 12 – medium heater; 13 – temperature regulator

In the general case, corrosion crack development in pipe steels at relative static loads is described by the diagram of static corrosion crack resistance (DSCCR) of this material under the appropriate corrosion-temperature conditions [1]. Figure 1 shows the schematic of such a diagram correlating growth rate  $v$  of normal tear corrosion crack with stress intensity factor  $K_I$ , determined by the stressed state, crack dimensions and sample geometry. In the general case, three characteristic zones are singled out on the DSCCR (see Figure 1), namely: I –  $0 < K_I < K_{ISCC}$ , where the crack growth rate is relatively low and anode dissolution of sample material in the crack tip is the main mechanism; II –  $K_{ISCC} < K_I < K_{IC}$  ( $K_{IC}$  is the  $K_I$  critical value at the given temperature conditions), where crack growth rate is considerable and the mechanism of hydrogen embrittlement of the material in the crack tip prevails; III –  $K_I < K_{IC}$ , where spontaneous crack growth corresponds to brittle fracture. In terms of ranking the detected corrosion crack, or its initiation, zone II is very important, determining the safe waiting period in the repair queue.

To obtain data on pipe steel behaviour in water solutions of various soils, PWI uses a procedure de-

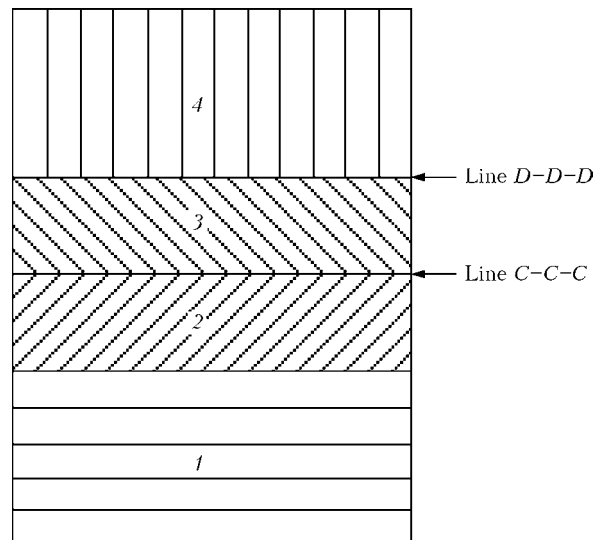


Figure 3. Schematic of characteristic regions on sample fracture surface (1-4 – see in the text)



scribed in [2, 3] allowing a sufficiently fast acquisition of information on DSCCR parameters in zone II, where crack growth proceeds in individual jumps, the presence of which is controlled with an acoustic emission transducer.

The purpose of this work was to confirm by the means of analytical scanning microscopy the working hypothesis of crack growth in the form of individual jumps, part of which are recorded as an acoustic emission signal on the screen and in the computer memory. In view of the selective nature of the process of hydrogenation of metal volumes along the crack front

through local dissociation of water solution in this zone, the jumps of crack growth along its front are of a local nature. Their displacement is quite chaotic – in spots along the front, from which layers are formed, determining the average rate of crack front movement.

Given below are the results of examination of fracture surface of 10 × 10 mm cross-section samples with Charpy notch and pre-grown crack. Testing was conducted by three-point bending (Figure 2) in the medium of aqueous extract of sand taken in different regions. Testing time for sample 1 was 740 h, for sample 2 it was 336 h. Samples were made from 17G1S

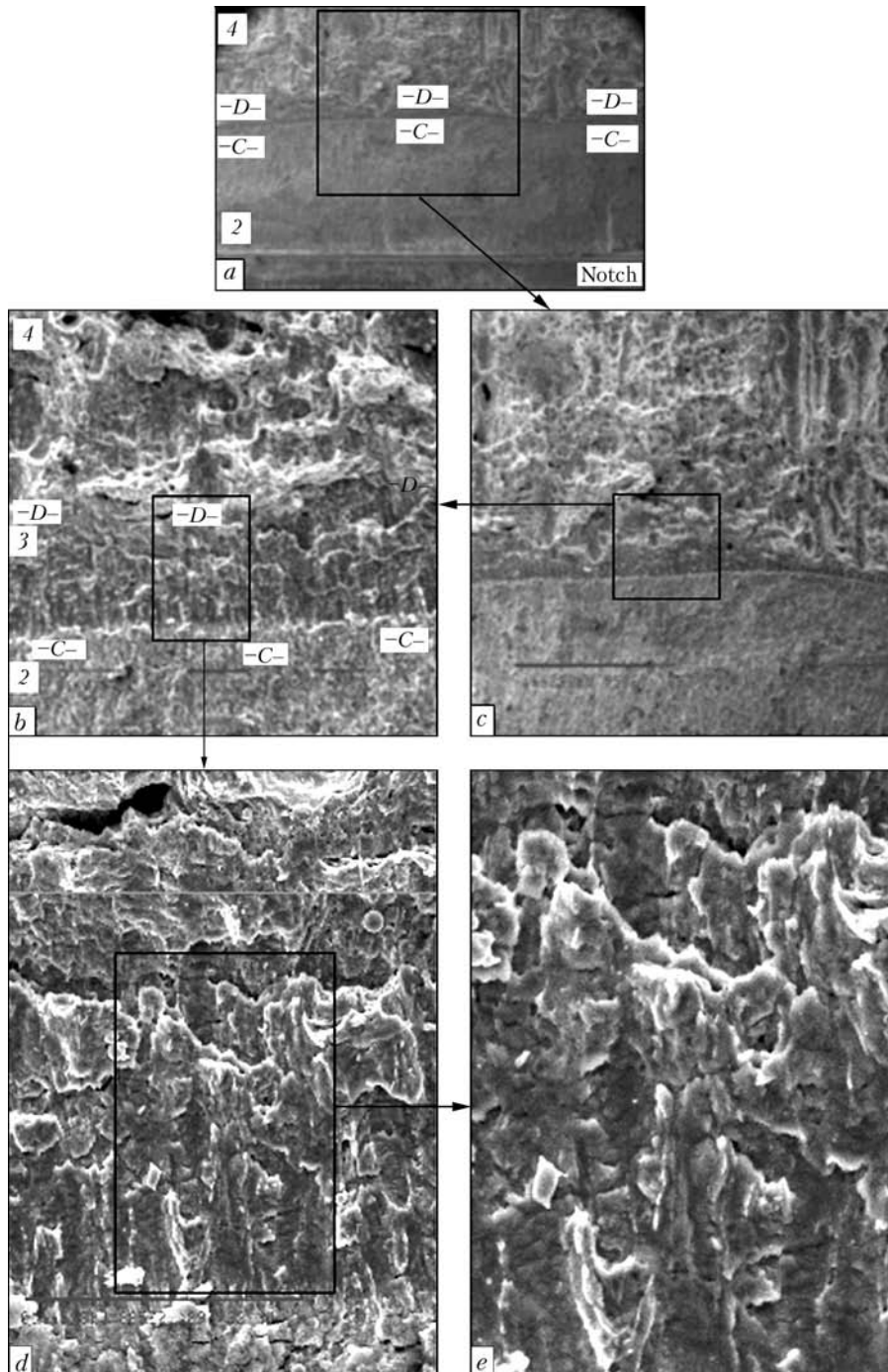


**Figure 4.** Fragments of fractographic examination of the region of growth of corrosion crack 3 in the section near the region of growth of fatigue crack 2 (a – ×28; b – ×221; c – ×55; d – ×885; e – ×1770)

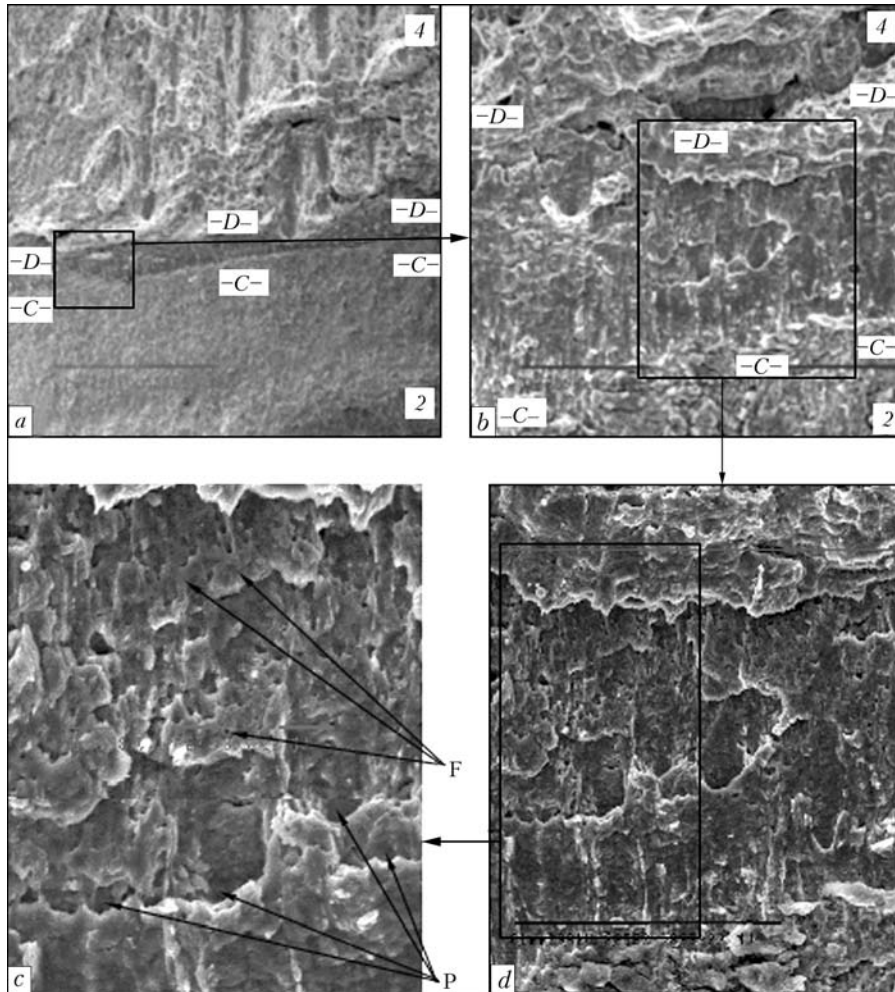


**Figure 5.** Fragments of fractographic examination of the region of corrosion crack growth near the final fracture region 4 (*a* –  $\times 555$ ; *b* –  $\times 442$  *c* –  $\times 1770$ ; *d* –  $\times 885$ ): F – quasibrittle fracture facets; P – flat pit in the extract zone

pipe steel. The following load was selected to achieve  $K_I = 25 \text{ MPa}\cdot\text{m}^{1/2}$ .

Fractures were studied using scanning electron microscope SEM-515 of Philips Company, fitted with energy dispersive spectrometers of «Link» system. Raster images of fracture surface structure enable producing a microimage with greater depth of the field of vision and getting a clearer view of structural details. Before conducting fracture surface examination, they were thoroughly cleaned from corrosion deposits using ultrasound. Four characteristic regions were found on fracture surfaces of each of the studied samples (Figure 3): 1 – notch region; 2 – region of pre-grown fatigue crack; 3 – region of bending deformations (i.e. corrosion crack growth), separating clear-cut region 2 and final fracture region 4. We are interested in the region separating regions 2 and 4. In sample 1 it is located between points D–D–D and C–C–C (Figures 4 and 5). Its width is 150–250  $\mu\text{m}$ , which agrees quite well with measurements under the objective of UIM-21 microscope on sample side surfaces before fracture. A system of quasibrittle fracture

facets is visible in the corrosion fracture zone, which form the above-mentioned layers (see Figures 4 and 5). Such a pattern was also found in sample 2. However, in connection with shorter testing time (336 h) the extent of the corrosion fracture region decreased to 70  $\mu\text{m}$ , and the quantity of conditional layers of corrosion crack growth was also reduced.

Thus, fracture morphology of tested samples demonstrates the acceptability of the concept of corrosion crack growing jump-like in hydrogen embrittlement zone, not simultaneously over the entire front, but in individual spots, moving quite chaotically along the front, yet still forming growth layers.

1. (2005) *Fracture mechanics and strength of materials: Refer. Book*. Ed. by V.V. Panasyuk. Vol. 7: Reliability and service life of structure elements of heat-and-power units. Ed. by I.M. Dmitrakh. Kyiv: Akadempriodika.
2. (2001) *Fracture mechanics and strength of materials: Refer. Book*. Ed. by Z.T. Nazarchuk. Vol. 5: Nondestructive testing and technical diagnostics. Lviv: G.V. Karpenko FMI.
3. Makhnenko, V.I., Shekera, V.M., Onoprienko, E.M. (2008) Determination of parameters of simplified static corrosion crack resistance diagram for pipe steels in soil corrosion. *The Paton Welding J.*, **10**, 26–30.